

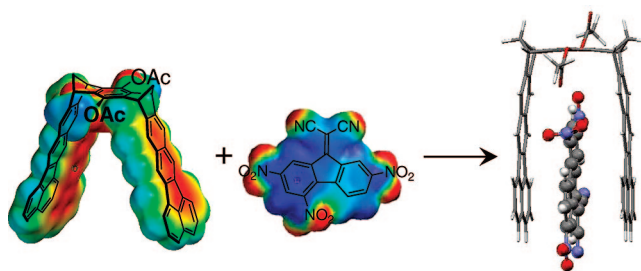
Molecular Clips with Extended Aromatic Sidewalls as Receptors for Electron-Acceptor Molecules. Synthesis and NMR, Photophysical, and Electrochemical Properties

Barbara Branchi,[†] Vincenzo Balzani,[†] Paola Ceroni,^{*,†} Mireia Campaña Kuchenbrandt,[‡] Frank-Gerrit Klärner,^{*,‡} Dieter Bläser,[‡] and Roland Boese[§]

Dipartimento di Chimica "G. Ciamician", Università di Bologna, via Selmi 2, I-40126 Bologna, Italy, and Institut für Organische Chemie and Institut für Anorganische Chemie der Universität Duisburg-Essen, Campus Essen, Universitätsstr. 5, 45117 Essen, Germany

paola.ceroni@unibo.it; frank.klaerner@uni-duisburg-essen.de

Received April 8, 2008



We have synthesized molecular clips **1** comprising (i) two benzo[*k*]fluoranthene sidewalls and (ii) a dimethylene-connected benzene bridge that carries two acetoxy (**1a**), hydroxy (**1b**), or methoxy (**1c**) substituents in the para position. Their NMR spectra, single-crystal structures, and photophysical (fluorescence intensity, lifetime, depolarization) and electrochemical properties are discussed. For the purpose of comparison, similar compounds (**2** and **3**) containing only one benzo[*k*]fluoranthene unit have been prepared and studied. The strongly fluorescent clips **1** form stable complexes with electron-acceptor guests because of a highly negative electrostatic potential on the inner van der Waals surface of their cavity. The complexation constants in chloroform solution for a variety of guests, determined by NMR and fluorescence titration, are much larger than those of the corresponding anthracene and naphthalene clips (**4** and **5**), particularly in the case of extended aromatic guests. The effect of the substituents in the para position of the benzene spacer unit of clips **1** is discussed on the basis of the host–guest complex structures obtained by X-ray analysis and molecular mechanics simulations. In the case of 9-dicyanomethylene-2,4,7-trinitrofluorene (TNF) guest, complex formation with clip **1a** causes dramatic changes in the photophysical and electrochemical properties: (i) a new charge-transfer band at 600 nm arises, (ii) a very efficient quenching of the strong benzo[*k*]fluoranthene fluorescence takes place, (iii) shifts of both the first oxidation (clip-centered) and reduction (TNF-centered) potentials are observed, and (iv) reversible disassembling of the complex can be obtained by electrochemical stimulation.

The design of efficient synthetic receptors¹ may be useful not only to selectively and efficiently recognize molecules or ions but also to better understand the structure and functionality of natural receptors. Molecular clips^{2–4} are very interesting host

species since they have a well-organized yet relatively flexible shape that enables interactions with guests of different size. The recognition process can be based on electron donor–acceptor interactions,⁵ hydrogen bonding,⁶ hydrophobic effects in aqueous media,⁷ ion pairing,⁸ and arene–arene interactions.⁹

[†] Università di Bologna.

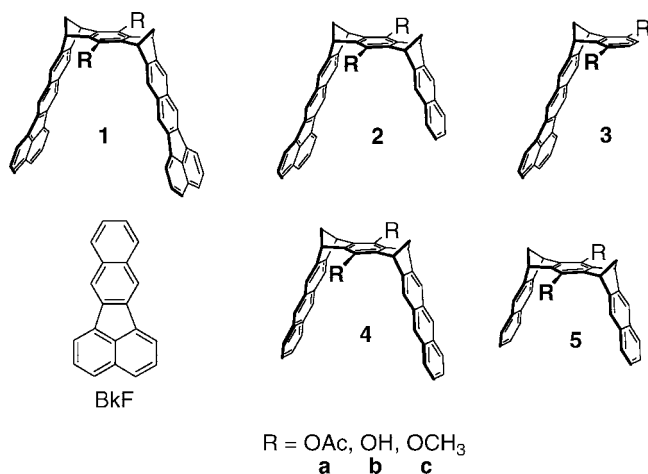
[‡] Institut für Organische Chemie der Universität Duisburg-Essen.

[§] Institut für Anorganische Chemie der Universität Duisburg-Essen.

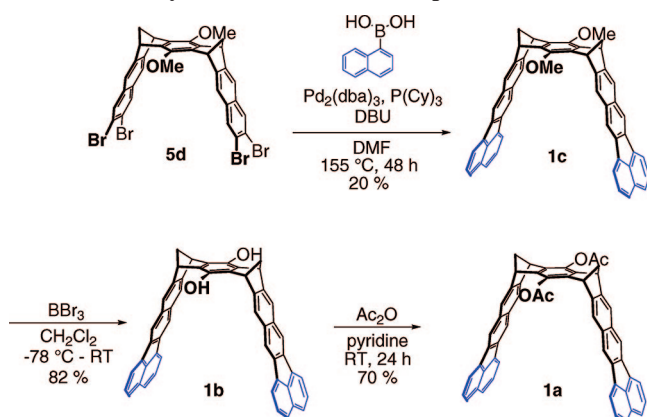
(1) For some recent reviews, see: (a) Schneider, H. J.; Yatsimirsky, A. K. *Chem. Soc. Rev.* **2008**, *37*, 263. (b) Biro, S. M.; Rebek, J. *Chem. Soc. Rev.* **2007**, *36*, 93. (c) Baldini, L.; Casnati, A.; Sansone, F.; Ungaro, R. *Chem. Soc. Rev.* **2007**, *36*, 254.

(2) (a) Klärner, F.-G.; Kahlert, B. *Acc. Chem. Res.* **2003**, *36*, 919. (b) Klärner, F. G.; Campaña Kuchenbrandt, M. Synthesis of molecular tweezers and clips by the use of a molecular Lego set and their supramolecular functions. In *Strategies and Tactics in Organic Synthesis*; Harmata, M., Ed.; Academic Press–Elsevier: Amsterdam, 2008; Vol. 7, Chapter 4. (c) Rowan, A. E.; Elemans, J.; Nolte, R. J. *Acc. Chem. Res.* **1999**, *32*, 995.

SCHEME 1. Structures of Benzo[*k*]fluoranthene (BkF), Molecular Clips 1, 2, 4, and 5, and Half-Clip 3



SCHEME 2. Synthesis of Molecular Clips 1a–c



Molecular tweezers and clips containing aromatic sidewalls² are able to form stable complexes with electron-deficient aromatic and aliphatic molecules, as well as inorganic and organic cations, including NAD⁺ (the important cofactor of many redox enzymes).¹⁰ The driving force for the formation of these adducts is based on charge-transfer interactions, coupled to CH– π and π – π interactions and, in some cases, electrostatic forces.

We have synthesized three molecular clips **1** (Schemes 1 and 2) containing extended aromatic sidewalls (namely, benzo[*k*]fluoranthene units). The two benzo[*k*]fluoranthene sidewalls are connected by a dimethylene-bridged spacer containing a benzene ring that carries two acetoxy (**1a**), hydroxy (**1b**), or methoxy (**1c**) substituents in the para position. Their NMR spectra, single-crystal structures, photophysical and electrochemical behavior, and host properties toward electron-deficient guest molecules have been investigated.

To elucidate the contribution of the expanded aromatic sidewalls to the binding of guest molecules, we also prepared molecular clip **2a** and half-clip **3a**, which contain only one benzo[*k*]fluoranthene sidewall, and we have compared the properties of the new compounds **1–3** with those of the

molecular clips **4** and **5**, which contain anthracene and naphthalene sidewalls, respectively.

The benzo[*k*]fluoranthene moieties have been selected because they are strongly fluorescent¹¹ polycyclic aromatic hydrocarbons with good electron-donor ability.¹² The resulting clips are soluble in organic solvents and present a highly negative electrostatic potential on the inner van der Waals surface of the cavity that forms a recognition site for electron-deficient guest molecules. Besides a thorough investigation of the novel compounds, we report the host–guest complex formation of clips **1–3** with different guest molecules substituted with electron-acceptor groups. The highly stable host–guest complex of clip **1a** with 9-dicyanomethylene-2,4,7-trinitrofluorene (TNF) has been studied in detail.

Results and Discussion

Synthesis of Molecular Clips 1a–c, 2a, and 3a. Starting from the known tetrabromonaphthalene clip **5d**,^{5a} the molecular clip **1c** with expanded benzo[*k*]fluoranthene sidewalls was prepared by a sequence of palladium-catalyzed Suzuki–Heck-type couplings with 1-naphthaleneboronic acid analogously to the coupling between 1,2-dibromobenzene and 1-naphthaleneboronic acid leading to fluoranthene.¹³ The dimethoxy-substituted clip **1c** was converted to the hydroquinone clip **1b** by reaction with boron tribromide and **1b** into the diacetoxy-substituted derivative **1a** by esterification of the hydroquinone **1b** with acetic anhydride.

Because the yield of the Suzuki–Heck-type coupling is only moderate (20%), we tried to synthesize clip **1a** with an independent route, namely, by repetitive Diels–Alder reactions of bisdienophile **8a** with two molecules of the *o*-quinodimethane derivative **7** (generated in situ by debromination of bis(dibromomethyl)fluoranthene **6**) followed by debromination of the Diels–Alder adduct analogously to the successful synthesis of molecular clips containing naphthalene sidewalls.¹⁴

Bis(dibromomethyl)fluoranthene **6** was prepared in three steps as shown in Scheme 3: (1) Diels–Alder cycloaddition of acenaphthylene to 2,3-dimethyl-1,3-butadiene, (2) oxidative dehydrogenation of the Diels–Alder adduct by the use of chloranil, and (3) photochemically induced *N*-bromosuccinimide

(4) Most recently, molecular clips have been used for the programmed synthesis of polycyclic nano objects: (a) Ghosh, S.; Mukherjee, P. *S Organometallics* **2008**, *27*, 316. (b) Ghosh, S.; Mukherjee, P. *S Dalton Trans.* **2007**, 2542. (c) Yang, H.-B.; Ghosh, K.; Das, N.; Stang, P. *J. Org. Lett.* **2006**, 3991.

(5) (a) Klärner, F. G.; Kahlert, B.; Boese, R.; Bläser, D.; Juris, A.; Marchioni, F. *Chem. Eur. J.* **2005**, *11*, 3363. (b) Marchioni, F.; Juris, A.; Lobert, M.; Seelbach, U. P.; Kahlert, B.; Klärner, F.-G. *New J. Chem.* **2005**, *29*, 780.

(6) Prins, L. J.; Reinhoudt, D. N.; Timmerman, P. *Angew. Chem., Int. Ed.* **2001**, *40*, 2383.

(7) Meyer, E. A.; Castellano, R. K.; Diederich, F. *Angew. Chem., Int. Ed.* **2003**, *42*, 1210.

(8) Gallivan, J. P.; Dougherty, D. A. *J. Am. Chem. Soc.* **2000**, *122*, 870.

(9) Hunter, C. A.; Lawson, K. R.; Perkins, J.; Urch, C. J. *J. Chem. Soc., Perkin Trans. 2* **2001**, 651.

(10) (a) Fokkens, M.; Jasper, C.; Schrader, T.; Koziol, F.; Ochsenfeld, C.; Polkowska, J.; Lobert, M.; Kahlert, B.; Klärner, F.-G. *Chem. Eur. J.* **2005**, *11*, 477–494. (b) Jasper, C.; Schrader, T.; Panitzky, J.; Klärner, F.-G. *Angew. Chem., Int. Ed.* **2002**, *41*, 1355–1358. (c) Klärner, F.-G.; Burkert, U.; Kamieth, M.; Boese, R. *J. Phys. Org. Chem.* **2000**, *13*, 604.

(11) Rivera-Figueroa, A. M.; Ramazan, K. A.; Finlayson-Pitts, B. J. *J. Chem. Educ.* **2004**, *81*, 242.

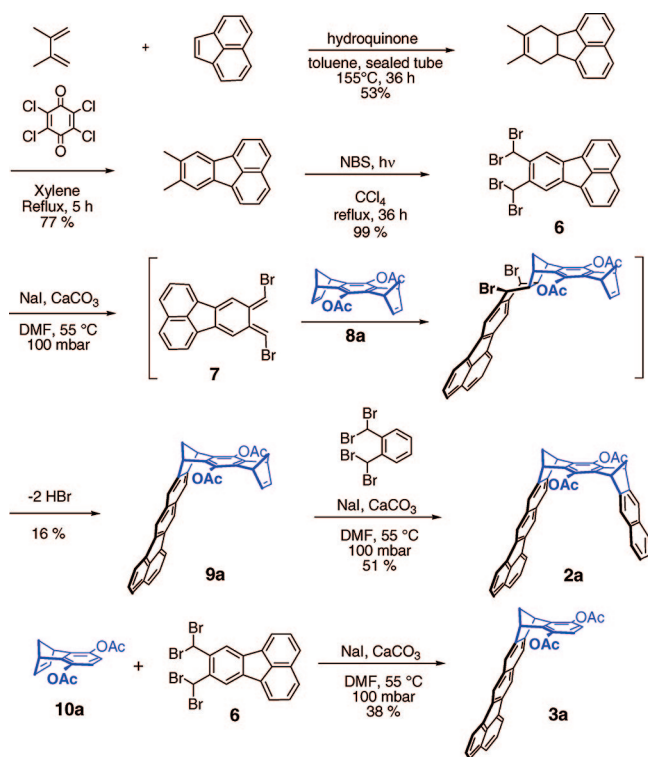
(12) Uibopuu, H.; Vodzinskii, Y. V.; Tikhova, N. Y.; Kirso, U.; Jacquignon, P. C. *Polynuclear Heterocyclic Hydrocarbons*; Plenum Publishing Corporation: New York, 1987; p 1233.

(13) Wegner, H. A.; Scott, L. T.; De Meijere, A. *J. Org. Chem.* **2003**, *68*, 883–887.

(14) Klärner, F.-G.; Panitzky, J.; Bläser, D.; Boese, R. *Tetrahedron* **2001**, *57*, 3573–3687.

(3) (a) Holder, S. J.; Elemans, J. A. A. W.; Donners, J. J. J. M.; Boerakker, M. J.; de Gelder, R.; Barberà, J.; Rowan, A. E.; Nolte, R. J. M. *J. Org. Chem.* **2001**, *66*, 391. (b) Shimizu, K. D.; Dewey, T. M.; Rebeck, J. J. *Am. Chem. Soc.* **1994**, *116*, 5145. (c) Zimmerman, S. C.; Wu, W.; Zeng, Z. *J. Am. Chem. Soc.* **1991**, *113*, 196. (d) Nedar, K. M.; Whitlock, H. W. *J. Am. Chem. Soc.* **1990**, *112*, 7269.

SCHEME 3. Synthesis of Clip 2a (Containing One Benzo[*k*]fluoranthene and One Naphthalene Sidewall) and “Half-Clip” 3a (Containing Only One Benzo[*k*]fluoranthene Sidewall)



(NBS) bromination produced the compound **6**. However, the reaction of **6** with the bisdienophile **8a** led only to the (1:1) adduct **9a**, even with a large excess of diene precursor **6**. Steric hindrance presumably prevents the annelation of a second expanded aromatic sidewall in **9a**, but this unexpected result allows us to isolate **9a** and to prepare the unsymmetrical clip **2a** by the reaction of **9a** with *o*-bis(dibromomethyl)benzene, which proceeds smoothly contrary to corresponding reaction with **6**. The “half clip” **3a** was prepared by the reaction of diacetoxybenzonorbornadiene **10a**¹⁵ with bis(dibromomethyl)fluoranthene **6** in the presence of sodium iodide and calcium carbonate analogously to **9a**. The structures of all new compounds were unambiguously characterized by their spectral data (see Experimental Section and Supporting Information). In the case of the diacetoxy-substituted clip **1a**, crystals could be grown that were suitable for a single-crystal structure analysis. Their analysis independently confirms the bowl-shaped structure of the clip molecule **1a**. In the crystal lattice of compound **1a**·2CHCl₃, two pairwise arranged clips are interpenetrating each other in an almost perpendicular fashion as shown in Figure 1. The main planes through the molecules form an interplanar angle of 78° [plane(C13, C51, C52, C37)/(C113, C151, C152, C137)] (see Experimental Section for the numbering of the carbon atoms) with the CHCl₃ groups filling gaps without obvious and specific interactions. The maximum distances of the sidewalls are similar (C13···C37 6.85 Å and C113···C137 6.97 Å), which is in the range of π stacked aromatic compounds. This highly ordered arrangement of intertwined clip molecules is evidently stabilized by intermolecular π - π stacking of the benzo[*k*]fluoranthene sidewalls.

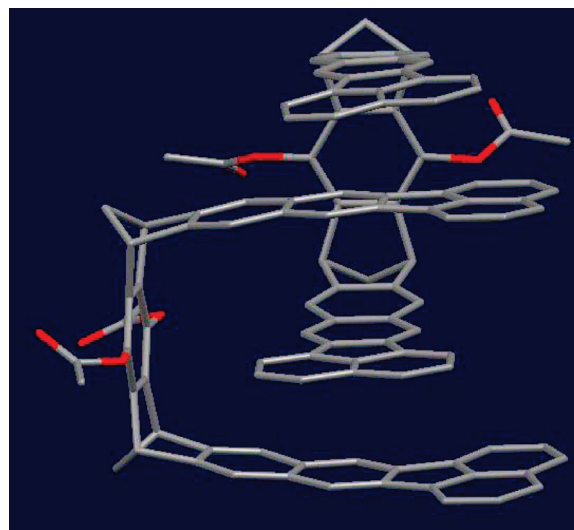


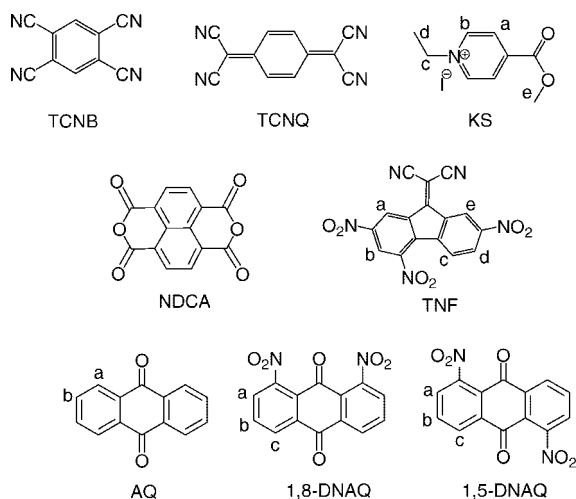
FIGURE 1. Two crystallographically independent molecules of **1a**·2CHCl₃ displayed as capped sticks without the CHCl₃ molecules, hydrogen atoms, and disorder.

The concentration dependence of ¹H NMR spectrum of **1a** in chloroform (CDCl₃), especially the concentration-dependent shift of the signal assigned to the central naphthalene protons (Figure S2 in the Supporting Information), indicates the formation of a weak self-assembled dimer (**1a**)₂ having an intertwined structure similar to that found in the crystal. With the assumption that the central naphthalene protons in (**1a**)₂ experience an upfield ¹H NMR shift similar to that ($\Delta\delta_{\text{max}} = 2.3$ ppm) found for the corresponding protons in the self-assembled dimer of the methanephosphonate-substituted clip having anthracene sidewalls,¹⁶ the binding constant can be estimated for the formation of (**1a**)₂ from the observed shift $\Delta\delta_{\text{obs}} = 0.05$ ppm to be $K_{\text{Dim}} = [(\mathbf{1a})_2]/[\mathbf{1a}]^2 \leq 10 \text{ M}^{-1}$. The missing concentration dependence of ¹H NMR spectra of the clips **1c** and **2a** indicate that these compounds exist monomolecularly-disperse in solution (Figures S3 and S4 in the Supporting Information).

Host–Guest Complex Formation. NMR Properties. The magnetic anisotropy of the clip arene units makes ¹H NMR spectroscopy a very sensitive probe for uncovering the binding of a guest molecule inside the clip cavity. The host–guest complex formation can be easily detected by pronounced upfield shifts of the ¹H NMR signals of the guest protons after addition of the clip as host molecule. In all binding processes reported here the host–guest association and dissociation are fast processes with respect to the NMR time scale. Thus, the maximum complexation-induced ¹H NMR shifts, $\Delta\delta_{\text{max}}$, of the guest signals ($\Delta\delta_{\text{max}} = \delta_0 - \delta_c$; where δ_0 , δ_c are the chemical ¹H NMR shifts of the protons of the free and complexed guest molecule, respectively) the association constants, K_a , and the free enthalpies of association, ΔG , could be determined by ¹H NMR titration. In these experiments the dependence of the complexation-induced ¹H NMR shifts, $\Delta\delta_{\text{obs}}$ ($\Delta\delta_{\text{obs}} = \delta_0 - \delta_{\text{obs}}$, where δ_{obs} is the chemical ¹H NMR shift of the guest proton observed in the presence of the host molecule and, hence, the weighted average between δ_0 and δ_c), of the guest signals from the host concentration, $[\text{H}]_0$, at constant guest concentration, $[\text{G}]_0 = \text{constant}$, is measured, as described in the Experimental Section. Scheme 4 shows the guest molecules studied in this work.

(15) (a) Vaughan, W. R.; Yoshimine, M. *J. Org. Chem.* **1957**, *22*, 7–12. (b) Meinwald, J.; Wiley, G. A. *J. Am. Chem. Soc.* **1958**, *80*, 3667–3671.

(16) Klärner, F.-G.; Kahlert, B.; Nellesen, A.; Zienau, J.; Ochsenfeld, C.; Schrader, T. *J. Am. Chem. Soc.* **2006**, *128*, 4831–4841.

SCHEME 4. Structures of Guest Molecules That Form Host–Guest Complexes with Molecular Clips^a


^a 1,2,4,5-tetracyanobenzene (TCNB), tetracyanoquinodimethane (TCNQ), Kosower salt (KS), 1,4,5,8-naphthalene-1,4,5,8-tetracarboxylic acid-dianhydride (NDCA), 9-dicyanomethylene-2,4,7-trinitrofluorene (TNF), anthra-9,10-quinone (AQ), 1,8-dinitroanthra-9,10-quinone (1,8-DNAQ), 1,5-dinitroanthra-9,10-quinone (1,5-DNAQ).

In the case of naphthalene-1,4,5,8-tetracarboxylic acid-dianhydride (NDCA), and 1,8- and 1,5-dinitroanthra-9,10-quinone (1,8- and 1,5-DNAQ), which are only slightly soluble in chloroform, it was not possible to determine the host–guest complex formation by conventional NMR titration experiments. Since the solubility of these molecules substantially increases in the presence of the molecular clip **1a** or **1c** by forming soluble host–guest complexes, the association constant, K_a , and the $\Delta\delta_{\max}$ values of the guest signals could be determined by solid–liquid extraction by means of ¹H NMR spectroscopy, as described in the Experimental Section. The host–guest complex between TNF and the diacetoxy-substituted clip **1a** is too stable for the determination of the K_a value by ¹H NMR titration. (The $\Delta\delta_{\text{obs}}$ values of the TNF protons are almost independent from the concentration of **1a** and close to the $\Delta\delta_{\max}$ value). In this case the binding constant, K_a , could be determined in more dilute solution either by spectrophotometric and spectrofluorimetric titration (vide infra).

Stoichiometry of Host–Guest Complexes. According to the analysis of the NMR titration experiments by the use of the HOSTEST program,¹⁷ TCNB and TCNQ form host–guest complexes of mixed (1:1) and (2:1) stoichiometry with the dimethoxy-substituted clip **1c**, whereas a (1:1) stoichiometry is

(17) HOSTEST v5.60; University of Pittsburgh: Pittsburgh, PA.

(18) The electrostatic potential surfaces (EPS) shown in Figure 2 were calculated by the use of computer program SPARTAN 04 Version 1.0.0 (Wavefunction Inc.) as described by Kamieth, M.; Klärner, F.-G.; Diederich, F. *Angew. Chem., Int. Ed.* **1998**, *37*, 3303–3306. Klärner, F. G.; Panitzky, J.; Preda, D.; Scott, L. *J. Mol. Model.* **2000**, *6*, 318–327.

(19) (a) Mohamadi, F.; Richards, N. G. J.; Guida, W. C.; Liskamp, R.; Lipton, M.; Caufield, C.; Chang, G.; Hendrickson, T.; Still, W. C. *J. Comput. Chem.* **1990**, *11*, 440–467. (b) *Macromodel*, v. 6.5; Schrödinger: Portland, OR.

(20) The dynamic processes, association–dissociation and guest rotation inside the host cavity, have been observed by the use of NMR spectroscopy at low temperatures. Lobert, M.; Bandmann, H.; Burkert, U.; Buchele, U. P.; Podosadowski, V.; Klärner, F.-G. *Chem.–Eur. J.* **2006**, *12*, 1629–1641.

(21) Mukherjee, T. K.; Levasseur, L. A. *J. Org. Chem.* **1965**, *30*, 644.

(22) (a) Hellrung, B.; Balli, H. *Helv. Chim. Acta* **1990**, *73*, 81. (b) Loufty, R. O.; Hsiao, C. K.; Ong, B. S.; Keoshkerian, B. *Can. J. Chem.* **1984**, *62*, 1877.

(23) (a) Binstead, R. A. *Specfit*; Spectrum Software Associates: Chapel Hill, NC, 1996. (b) Gampp, H.; Maeder, M.; Meyer, C. J.; Zuberbulher, A. *Talanta* **1985**, *32*, 257.

(24) Förster, Th. *Discuss. Faraday Trans* **1959**, *27*, 7.

TABLE 1. Association Constants (K_a) Determined for the Formation of Host–Guest Complexes with 1:1 Stoichiometry^a

guest	K_a (M^{-1})	
	host 1a (R = OAc)	host 1c (R = OMe)
TCNB	9.2×10^2	4.4×10^{2b} ; 1.6×10^2
TCNQ	5.8×10^2	2.3×10^{2b} ; 1.2×10^2
KS	4.8×10^2	5.0×10
NDCA	3.5×10^{4c} ; 6.3×10^{4d}	1.2×10^{4c}
TNF	2.5×10^{5d} ; 3.3×10^{5e}	6.9×10^3
AQ	4.4×10	
1,8-DNAQ	4.7×10^{3c}	2.3×10^{3c}
1,5-DNAQ	5.0×10^{3c}	2.7×10^{3c}

^a Unless otherwise noted, determined by ¹H NMR titration experiments in chloroform at 298 K. ^b Association constant for the 2:1 host:guest complex. ^c Determined by solid–liquid extraction. ^d Determined by spectrofluorimetric titration (see below), ^e Determined by spectrophotometric titration (vide infra).

found for all other complexes by this kind of analysis (Table 1). A single-crystal structure analysis of the crystalline complex between the dimethoxy clip **1c** and TCNB shows a (2:1) host–guest stoichiometry supporting the results in solution (vide infra).

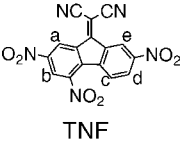
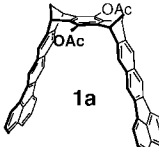
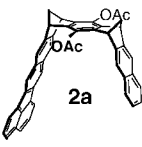

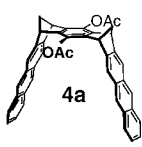
Stability of Host–Guest Complexes. The data summarized for the host–guest complex formation of the benzo[*k*]fluoranthene clips **1a,c** in Table 1 allow the following conclusions: (i) all complexes of the diacetoxy-substituted clip **1a** are more stable than the corresponding ones of the methoxy-substituted clip **1c**; (ii) the complexes of the benzo[*k*]fluoranthene clips **1a,c** are more stable than the corresponding complexes of the anthracene or naphthalene clips **4a,c** or **5a,c**.

The effect of the substituents at the central spacer unit has previously been observed for clips **4a,c** or **5a,c**.^{5,14} It has been explained by their different steric size and conformations with respect to the clip cavity. In the case of the dimethoxy-substituted systems, the *syn,syn* conformation (in which both OMe groups point toward the clip cavity) is calculated by force field to be the preferred one. In this conformation the sterically relatively large OMe substituents shield the clip cavity and, hence, disfavor the complex formation. In the case of the diacetoxy-substituted system **5b** the *anti,anti* conformation was calculated to be the most stable one. In this conformation there is no steric hindrance to complex formation. In the single-crystal structures of some complexes of the diacetoxy-substituted naphthalene clip **5a** a *syn,anti* conformation is observed in which the carbonyl oxygen atom (pointing toward the cavity) obviously forms an additional attractive interaction with the guest molecule.

The higher stability of the host–guest complexes of the benzo[*k*]fluoranthene clips **1a,c** with respect to the corresponding complexes of the anthracene or naphthalene clips **4a,c** or **5a,c** can be rationalized with the larger van der Waals contact surface of the benzo[*k*]fluoranthene sidewalls in the molecular clips of type 1 compared to the anthracene or naphthalene sidewalls in the clips of type 4 or 5. This stabilizing effect is relatively small in the case of the monocyclic guest molecules such as TCNB, TCNQ, and Kosower salt (KS, Scheme 4). The complexes of **1a** with these guest molecules are only more stable by a factor of 1.3–4.5 or 3.4–19.3 than the corresponding complexes of the anthracene clip **4a** or the naphthalene clip **5a**.

A dramatic increase (by a factor ≥ 500) in the stability of the TNF complex with **1a** compared to that with the anthracene clip **4a** (Table 2) was found. The comparison of the binding constant of complex **1a**⊃TNF with that of **2a**⊃TNF or **3a**⊃TNF

TABLE 2. Maximum Complexation-Induced ^1H NMR Shifts of TNF Protons, $\Delta\delta_{\text{max}}$, and Association Constants, K_a , for the Formation of the TNF complexes of **1a**, **2a**, **3a**, and **4a**^a

Guest	Host			
	1a	2a	3a	4a
				
guest TNF	host			
K_a	2.9×10^{5b}	6.1×10^2	1.2×10^2	5.7×10^2
$\Delta\delta_{\text{max}}$ H _a	1.6	1.6	2.0	1.1
$\Delta\delta_{\text{max}}$ H _b	<i>c</i>	1.0	1.2	0.6
$\Delta\delta_{\text{max}}$ H _c	2.1	1.9	1.4	2.7
$\Delta\delta_{\text{max}}$ H _d	<i>c</i>	2.4	1.3	2.8
$\Delta\delta_{\text{max}}$ H _e	1.9	1.6	1.8	1.2

^a Determined by ^1H NMR titration experiments in CDCl_3 at 298 K. ^b Mean value obtained from spectrofluorimetric and spectrophotometric titration. ^c Not detectable.

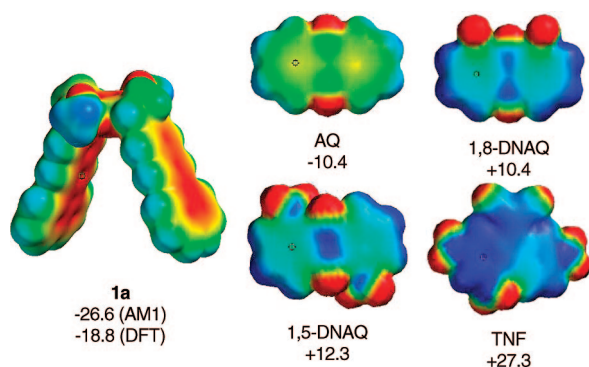


FIGURE 2. Electrostatic potential surfaces (EPSs) of the diacetoxy-substituted benzo[*k*]fluoranthene clip **1a** (left) and guest molecules (right) calculated by AM1. The color code spans from -25 kcal/mol (red) to $+25$ kcal/mol (blue). The listed molecular electrostatic potentials (MEP in kcal/mol) were calculated at the marked positions by AM1 and in the case of **1a** additionally by B3LYP/6-31G**//AM1.²⁵ Both methods led to highly negative MEP values.

demonstrates that both benzo[*k*]fluoranthene sidewalls in **1a** are essential for the formation of this extraordinarily stable host–guest complex. Finally, the finding that the complexes of the dinitro-substituted anthra-9,10-quinone derivatives (1,8- and 1,5-DNAQ) with molecular clip **1a** are substantially more stable than that of the parent anthra-9,10-quinone (AQ, Table 1) allows the conclusion that electron donor–acceptor interactions provide an important contribution to the host–guest binding in these systems despite their large van der Waals contact surfaces. The electrostatic potential surfaces (EPS calculated by quantum chemical methods) show the complementary nature of the negatively polarized host cavity and the positively polarized guest molecules substituted by electron-withdrawing nitro or cyano groups leading to the tight binding of 1,5-DNAQ, 1,8-DNAQ, and TNF by molecular clip **1a**, whereas the EPS of the benzene rings of anthra-9,10-quinone (AQ) is still slightly negative though this molecule contains the electron-withdrawing carbonyl functions (Figure 2). The negatively polarized AQ is only weakly bound to **1a**.

Complex Structures Calculated by Molecular Mechanics. The large complexation-induced shifts of the ^1H NMR signals,

$\Delta\delta_{\text{max}}$, of the guest protons in the complexes of the molecular clips **1a,c** (Table 2 and Table S1 in the Supporting Information) are of comparable size to those observed in corresponding complexes of the clips **4a,c** and **5a,c** containing the smaller anthracene or naphthalene sidewalls. This finding indicates that in all these complexes with **1a,c**, **4a,c**, and **5a,c** the guest molecules are positioned inside the clip cavity similarly. The complex structures (calculated by force field using a Monte-Carlo conformer search, Figure 3) agree well with the observed large $\Delta\delta_{\text{max}}$ values which are affected by the magnetic anisotropy of the surrounding clip arene-units (Figure 4).

The calculated structures show that in the case of the monocyclic guest molecules such as TCNB or TCNQ only the upper naphthalene units of the benzo[*k*]fluoranthene sidewalls are needed for the binding of the guest molecule, whereas in the case of the larger polycyclic guest molecules such as NDCA, TNF, etc. the complete benzo[*k*]fluoranthene sidewalls are used for the binding of the guest molecule. This certainly explains why the increase in the stability of the complexes with **1a,c** is much larger with the polycyclic guest molecules than that found for the smaller monocyclic guest molecules. According to the calculations (Figure 3), the chemically equivalent protons in the free guest molecules are expected to be nonequivalent in the host–guest complexes each showing two separated ^1H NMR signals. The observation of only one ^1H NMR signal for the bound guest molecule such as TCNB, TCNQ, or NDCA provides evidence that the mutual complex dissociation–association, as well as the rotation of the guest molecule inside the clip cavity, are fast processes with respect to the NMR time scale. Thus, only one signal as average of the signals of all possible conformers is observed.²⁰ This result confirms the assumption which has been made for the analysis of the ^1H NMR titration experiments. The finding of similar $\Delta\delta_{\text{max}}$ values for the TNF protons H_a, H_c, and H_e in the highly stable complex **1a**⊃TNF (Table 2) indicates that this complex exists as a dynamic equilibrium between both conformers shown in Figure 3 contrary to complex **4a**⊃TNF, which seems to exist mainly in the higher energy conformer according to the larger $\Delta\delta_{\text{max}}$ values found for the TNF protons H_c and H_d.^{5a}

Single Crystal Structure of a Host–Guest Complex. The single-crystal structure determined for the (2:1) complex between the dimethoxy-substituted clip **1c** and TCNB as guest molecule displays a different position of the guest molecule. In

(25) Debad, J. D.; Morris, J. C.; Magnus, P.; Bard, A. J. *J. Org. Chem.* **1997**, *62*, 530.

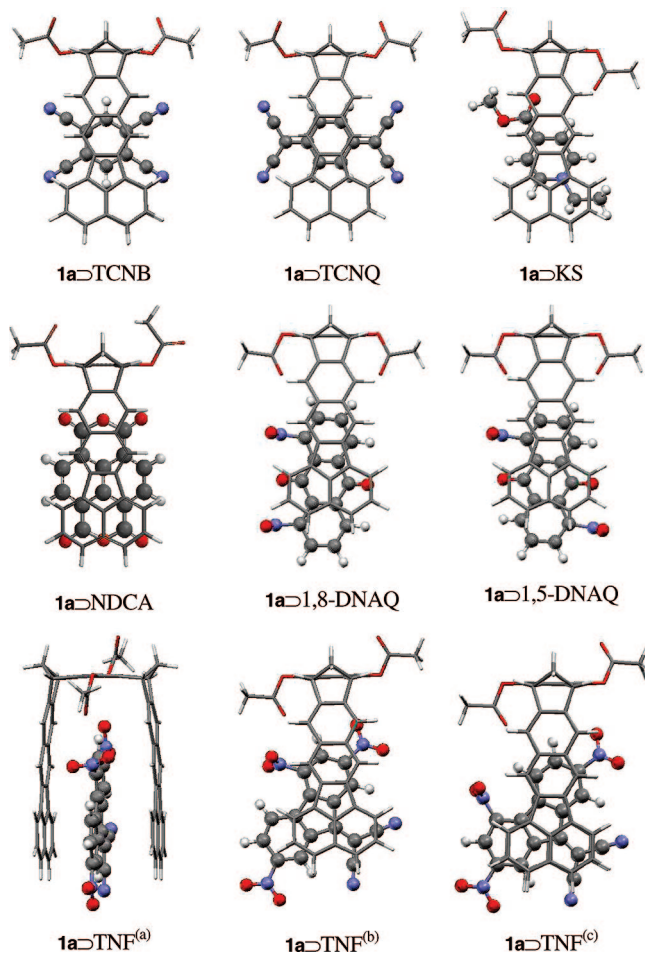


FIGURE 3. Lowest energy structures of the host-guest complexes of the diacetoxy-substituted clip **1a** with various guest molecules calculated by a Monte-Carlo conformer search (MacroModel 6.5, force field: AMBER*, 5000 structures):¹⁹ (a) front view and (b) side view of the energy minimum structure of complex **1a**⊃TNF; (c) side view of a structure calculated to be higher in energy by 3.7 kcal/mol.

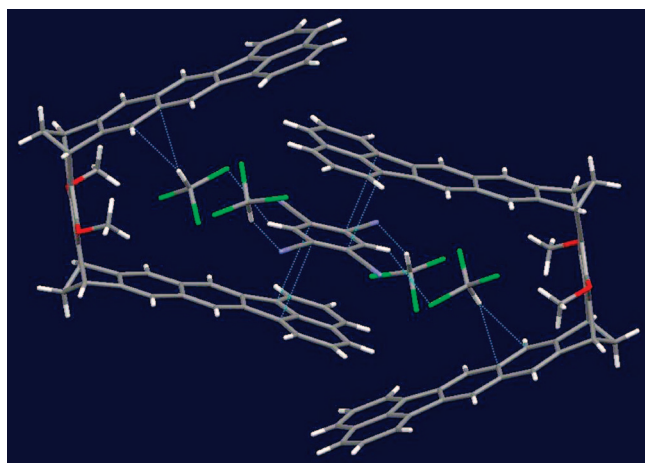


FIGURE 4. Clips in **1c**·1/2TCNB ($C_{10}H_2N_4$)·2CHCl₃ displayed as capped sticks with blue lines between the side walls indicating the π -stacking (C32...C74 3.37 Å) and the C-H... π interactions from the CHCl₃ molecules (H71...C45 2.61 Å) and to the TCNB (H60...N2 2.53 Å).

this structure (formally consisting of **1c**·1/2TCNB ($C_{10}H_2N_4$)·2CHCl₃) where TCNB is additionally complexed between the sidewalls of two pairwise and centrosymmetric arranged

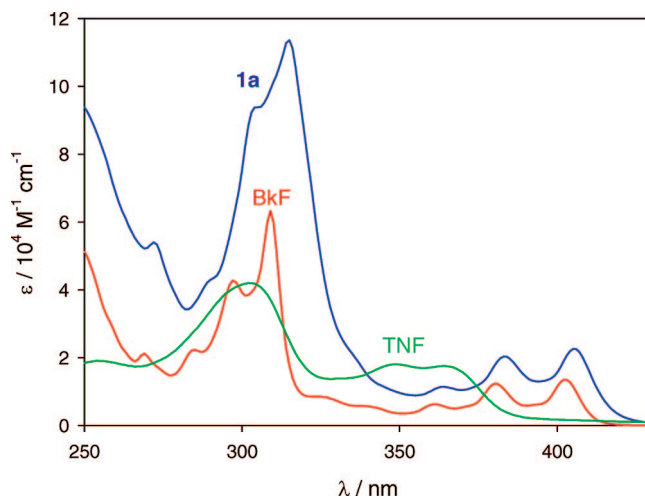


FIGURE 5. Absorption spectra of compounds **1a**, BkF, and TNF in CHCl₃ solution.

clips, the walls are bent outward. Thus, they can adopt the TCNB between one sidewall of each clip. The high flexibility of the clips is apparent due to the expansion by 4.7 Å (distance C4...C28 11.36 Å). Two of the CHCl₃ molecules are situated inside the clips where they employ C-H...Cl and C-H... π contacts (2.82 and 2.61 Å). The CHCl₃ molecules outside the clips are linked via C-H...N contacts (2.53 Å) (Figure 5). The two methoxy groups attached to the central spacer unit of **1c** point toward the clip cavity and evidently shield the upper part of the cavity from binding the TCNB molecule in this part of the clip cavity. This observation may explain why **1c** also forms (2:1) complexes with the small guest molecules TCNB and TCNQ in solution.

Photophysical Properties. The benzo[*k*]fluoranthene chromophore presents two structured $\pi\pi^*$ bands with maximum at 309 and 404 nm in CHCl₃ solution at room temperature (Figure 5).¹⁰

The absorption spectra of the two clips **1a,c** are similar to that of model compound BkF with slightly broader and red-shifted bands. The molar absorption coefficients of clips **1a** and **1c** (Table 3) are lower than expected, taking into account that each molecule contains two chromophores. This effect may be due to a perturbation of the chromophore properties upon functionalization with the bridge, while a through-space interaction of the two chromophores is not likely because of the distance and quite low flexibility of the bridge. Compounds **1a,c** and BkF are highly fluorescent (Figure 6 and Table 3) with a structured band with $\pi_{\max} \approx 415$ nm. In the case of the two clips, the emission band is slightly red-shifted and corresponds to a smaller quantum yield compared to BkF, while the lifetime of the emitting excited-state is the same for the three compounds. These results suggest slight differences in the radiative and nonradiative rate constants of the fluorescent excited-state in going from BkF to clips **1a** and **1c**. At 77 K in CH₂Cl₂/CHCl₃ 1:1 (v/v) rigid matrix, the emission spectra of the three compounds show a slightly blue-shifted fluorescent band and a structured and much weaker phosphorescence with $\pi_{\max} = 568$ nm and lifetime $\tau = 0.4$ s (Table 3, Figure 6).

No evidence of concentration dependence of either absorption or emission spectra of **1a** and **1c** confirms that in dilute solutions this molecular clip exists as a monomer (vide supra).

TNF shows two absorption bands at 310 and 350 nm, a tail extending up to 450 nm (green line in Figure 5), and a very

TABLE 3. Photophysical Data in Air-Equilibrated CHCl₃ Solution, unless Otherwise Noted

	298 K					77 K ^a			
	absorption		fluorescence			fluorescence		phosphorescence	
	λ_{\max} (nm)	ϵ (10 ⁴ M ⁻¹ cm ⁻¹)	λ_{\max} (nm)	Φ_{em}	τ (ns)	λ_{\max} (nm)	τ (ns)	λ_{\max} (nm)	τ (s)
1a	405	2.3	415	0.5	7.0	412	7.0	568	0.4
1c	405	1.8	415	0.5	7.0	412	7.0	568	0.4
BkF	402	1.3	412	0.7	7.0	408	7.0	568	0.4
TNF	364	1.8	530	10 ⁻³	0.8				

^a Emission spectra performed in CH₂Cl₂/CHCl₃ 1:1 (v/v).

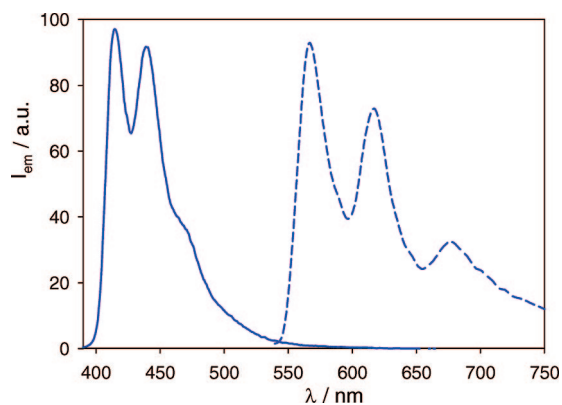


FIGURE 6. Fluorescence (solid line, CHCl₃ solution, 298 K) and phosphorescence (dashed line, CH₂Cl₂/CHCl₃ 1:1 v/v, 77 K) spectra of compounds **1a**. $\lambda_{\text{ex}} = 380$ nm.

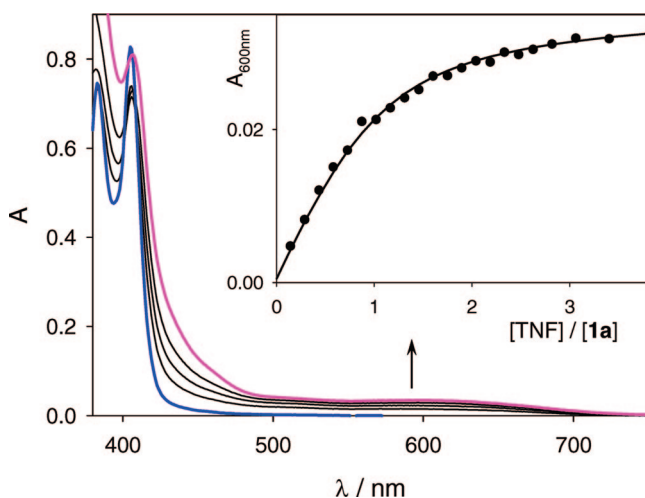


FIGURE 7. Absorption spectral changes upon titration of a 7.2×10^{-6} M solution of **1a** with TNF in CHCl₃ solution (cuvette optical path = 5 cm). Blue and pink lines correspond to the addition of 0 and 3 equiv of TNF per clip, respectively. The inset shows the absorbance changes at 600 nm with the fitting curve obtained by Specfit.²⁷

weak fluorescence band at 530 nm (Table 3). Upon titration of a 7.2×10^{-6} M CHCl₃ solution of **1a** with a 2×10^{-3} M CHCl₃ solution of TNF, a new absorption band at 600 nm increases (Figure 7), and concomitantly the fluorescence intensity of the clip, upon excitation at the 402 nm isosbestic point, decreases (Figure 8).

Global fitting of the changes in the absorption spectra show that a 1:1 adduct with $K_a = 3.2 \times 10^5$ M⁻¹ and $\tau = 1000$ M⁻¹

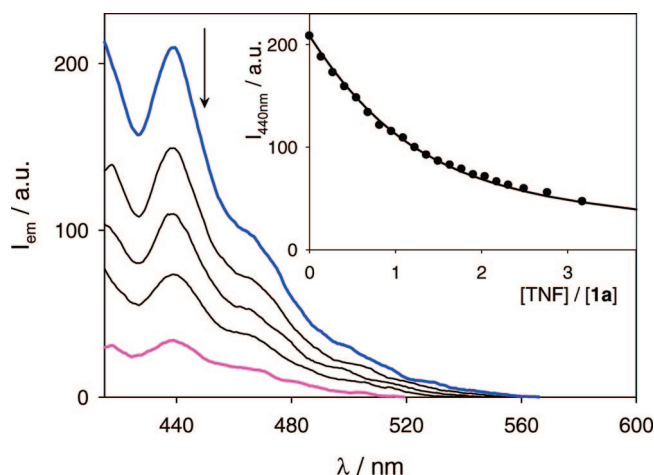


FIGURE 8. Fluorescence spectral changes upon titration of a 4.4×10^{-6} M solution of TNF with **1a** in CHCl₃ solution. Blue and pink lines correspond to the addition of 0 and 3 equiv of TNF per clip, respectively. The inset shows the emission intensity changes at 440 nm and the fitting curve obtained by Specfit.²²

cm⁻¹ at 600 nm is formed. The fitting of the emission spectra with the same procedure yields a similar value within the experimental error: $K_a = 2.5 \times 10^5$ M⁻¹. As previously discussed, the formation of the **1a**⊃TNF adduct is due to electron donor–acceptor interactions between the strong electron-acceptor guest^{21,22} (see also electrochemical experiments below) and the electron-donating cavity of the clip. The formation of a complex with charge transfer (CT) character is consistent with both the presence of a low-energy CT absorption band with maximum at 600 nm and the quenching of the fluorescent excited-state of the benzo[*k*]fluoranthene moiety of the clip. The CT band resulting from the complex formation is responsible for the color change from yellow to green (Figures 5 and 7) of the solution containing clip **1a** upon addition of TNF. A color change is also observed upon titration of clip **1a** with other guest molecules, for example, with NDCA the color changes from yellow to red.

No change in the photophysical properties of BkF has been observed upon addition of up to 10 equiv of TNF in CHCl₃ solution, demonstrating that the supramolecular structure of clip **1a** is necessary for the formation of a stable adduct with high association constant.

Fluorescence Anisotropy. The fluorescence anisotropy is defined as

$$r = (I_{\parallel} - I_{\perp}) / (I_{\parallel} + 2I_{\perp}) \quad (1)$$

where I_{\parallel} and I_{\perp} are the emission intensities registered when the emission and excitation polarizers are oriented parallelly or perpendicularly, respectively. For a single molecular species in a rigid matrix, the fluorescence anisotropy corresponds to an

(26) Kaifer, A. E.; Gómez-Kaifer, M. *Supramolecular Electrochemistry*; Wiley-VCH: Weinheim, 1999; Chapter 9.

(27) The nonlinear regression analyses of the NMR titration experiments were performed by means of the computer program *TableCurve 2D 5.0I*; SYSTAT Software, Inc.: Richmond, CA.

TABLE 4. Steady-State Fluorescence Anisotropy Values (r_{ss}) and Rotational Relaxation Times (θ)^a

CHCl ₃ /propylene glycol	r_{ss}	θ (ns)
1a		
1:1	0.02	9
1:1	(0.2) ^b	
1:99	0.08	
1c		
1:1	0.02	8
1:1	(0.2) ^b	
1:99	0.08	
		BkF
1:1	0.01	2
1:1	(0.3) ^b	
1:99	0.05	

^a In air-equilibrated CHCl₃/propylene glycol mixtures at 298 K, unless otherwise noted. ^b Steady-state fluorescence anisotropy in CHCl₃/CH₂Cl₂ 1:1 (v/v) at 77 K.

intrinsic value r_0 that depends only on the different orientation of the absorption and emission transition moments. In the case of a fluid solution, the value of the anisotropy decreases if the molecule undergoes a change in orientation during the excited-state lifetime. In particular, in the case of a spherical rotor, the decay of r can be fitted by a monoexponential model (eq 2)

$$r(t) = r^0 e^{-t/\theta} \quad (2)$$

where θ is the rotational relaxation time, which can be related to the hydrodynamic volume V_h by the Stokes–Einstein–Debye equation:

$$\theta = \frac{V_h \eta}{k_B T} \quad (3)$$

where η is the viscosity of the solvent, k_B is the Boltzmann constant, and T is the absolute temperature.

For species containing only a fluorophoric unit as BkF, the value of the rotational relaxation time (θ) in fluid solution yields information on the hydrodynamic volume (V_h) of the molecule. On the other hand, for clips **1a** and **1c**, which contain two identical fluorophoric units, fluorescence depolarization can occur also by energy migration from the originally excited unit to the other differently oriented one. The single-crystal structure of clip **1a** shows that the two benzo[*k*]fluoranthene moieties of the clips are not randomly oriented because of the constraint imposed by the central spacer unit. However, the symmetrical geometry of the clips does not imply a collinear orientation of the emission transition moments of the two fluorophores, so that energy migration may, in principle, cause fluorescence depolarization.

The measurements in fluid solution were performed in CHCl₃/propylene glycol mixtures, because in the low-viscosity CHCl₃ solvent, complete depolarization takes place during the excited-state lifetime for compounds **1a,c** and BkF, while in pure propylene glycol the investigated compounds are not soluble. Experimental data reported in Table 4 show that (i) no significant difference has been observed for **1a** and **1c**, as expected; (ii) r_{ss} and θ values are higher for the clips compared to BkF in fluid solution; (iii) the steady-state fluorescence anisotropy measured in a rigid matrix of CH₂Cl₂/CHCl₃ 1:1 (v/v) at 77 K is lower for the clips compared to BkF. These results suggest that in fluid solution fluorescence depolarization of the clip takes place by two channels, namely, rotation and energy migration, whereas in the case of BkF only the former channel is present, but with a higher efficiency due to the lower hydrodynamic volume of

the compound. The r_{ss} values obtained in rigid matrix reflect the intrinsic anisotropy r_0 for BkF but not for clips **1a** and **1c**. Indeed, the r_0 value is the same for the benzo[*k*]fluoranthene chromophore isolated or inside the clip structure, and the lower value of r_{ss} in rigid matrix for **1a** and **1c** is due to fluorescence depolarization by energy migration. On the other hand, in fluid solution the situation is opposite: the values of r_{ss} are higher for clips **1a** and **1c** compared to BkF. This result can be rationalized considering that, under these experimental conditions, the main mechanism of depolarization is rotation for all of the investigated compounds and that rotation is slower for the clips because of their higher hydrodynamic volume. This hypothesis is also confirmed by the fact that, upon decreasing the solvent viscosity, i.e., in going from CHCl₃/propylene glycol 1:99 to 1:1 (v/v) mixtures, a decrease of ca. 4 times in the steady-state anisotropy has been observed for both BkF and the clips and that complete depolarization takes place in pure CHCl₃ solution. As to the fluorescence anisotropy decay, the experimental data can be fitted considering an apparent r_0 value of 0.20 for the clips and an r_0 value of 0.30 for BkF. Indeed, depolarization by energy migration takes place on a much shorter time-scale that cannot be investigated with our experimental setup. Energy migration is a very fast process of depolarization since, based on the Förster theory:²⁴ (i) $k_{en} = 10^{11} \text{ s}^{-1}$ for a distance of 1 nm between the two fluorophores of the clips, compared to an intrinsic deactivation rate constant $k = 1/\tau = 1.1 \times 10^8 \text{ s}^{-1}$ ($\tau = 9 \text{ ns}$ in CHCl₃/propylene glycol 1:99 v/v); (ii) the distance value where the rate of energy transfer and that of intrinsic deactivation are equal (R_0) is 3 nm. Therefore, fluorescence anisotropy decay observed in the ns time scale for compounds **1a,c** and BkF at 298 K is due to depolarization by rotation and can thus be correlated with the corresponding hydrodynamic volumes.

Electrochemical Properties. The oxidation of BkF is known to be associated with a dimerization reaction. In particular, the (7,12-diphenyl)benzo[*k*]fluoranthene undergoes a dimerization process upon oxidation: a dimer is formed upon removal of two electrons and two hydrogen atoms.²⁵

Cyclic voltammograms performed on benzo[*k*]fluoranthene and **1a** in CH₂Cl₂/TBAPF₆ solutions at 298 K show no reduction process in the available negative potential window and oxidation processes (Figure 9a and Table 5) with partial chemical irreversibility.

In the case of BkF, chemical reversibility for the one-electron oxidation process is achieved at 1 V/s, although the corresponding $E_{1/2}$ value reported in Table 5 is partially affected by adsorption phenomena upon the reverse cathodic scan. The clip **1a** presents three oxidation processes: the first two processes are one-electron transfers associated to chemical reactions. They likely correspond to the first oxidation of each benzo[*k*]fluoranthene in the clip occurring at distinct potential values because of electrostatic and/or electronic interactions between the two moieties: the first is oxidized at less positive potential and the second at approximately the same value as that observed for benzo[*k*]fluoranthene. Upon increasing the scan rate, the height of the reverse peaks at ca. 1.2 V (vs SCE) in Figure 9a increases in intensity and that of the peak at 1.05 V (vs SCE) decreases, indicating that the last process corresponds to the rereduction of a product formed by the chemical reaction coupled to the first two electron transfer processes. Complete chemical reversibility is not observed even at scan rates of 20 V/s. The third

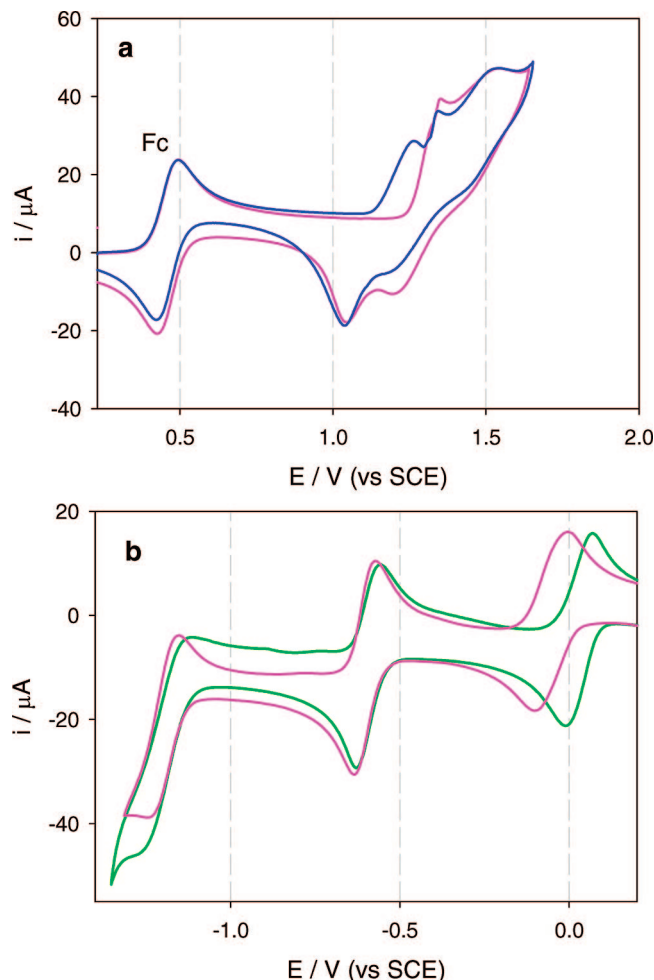


FIGURE 9. Cyclic voltammograms of compounds **1a** (blue line) and TNF (green line) and an equimolar solution of **1a** and TNF (pink line) with concentration of 1.3 mM in $\text{CH}_2\text{Cl}_2/\text{TBAPF}_6$ solution. Working electrode, glassy carbon; scan rate, 0.05 V/s. In panel a, ferrocene (Fc) reversible oxidation is also reported.

TABLE 5. Electrochemical Data in $\text{CH}_2\text{Cl}_2/\text{TBAPF}_6$ Solution at 298 K

	III_{red}	II_{red}	I_{red}	I_{ox}	II_{ox}	III_{ox}
1a				+1.28	+1.33	+1.55 ^a
BkF				+1.33 ^b		
TNF	-1.19	-0.62	-0.02			
1a ⊃TNF	-1.19	-0.62	-0.12		+1.33 ^c	+1.55 ^a

^a Chemically irreversible process; E_{pa} value at 0.2 V/s. ^b Adsorption on the working electrode partially affects the reverse scan. ^c Bielectronic process.

electron transfer process is broader and chemical irreversible, thus precluding a careful estimation of the number of electrons exchanged.

Under the same experimental conditions, TNF shows three reversible one-electron reduction processes (green line in Figure 9b, Table 5): the first process occurs at -0.02 V (vs SCE) demonstrating the strong electron-acceptor character of this compound.²² No oxidation process is observed in the available potential window.

An equimolar solution of **1a** and TNF ($c = 1.3$ mM) in $\text{CH}_2\text{Cl}_2/\text{TBAPF}_6$ shows cyclic voltammograms in which the first oxidation process is positively shifted (pink line in Figure 9a) and the first reduction process is negatively shifted (pink

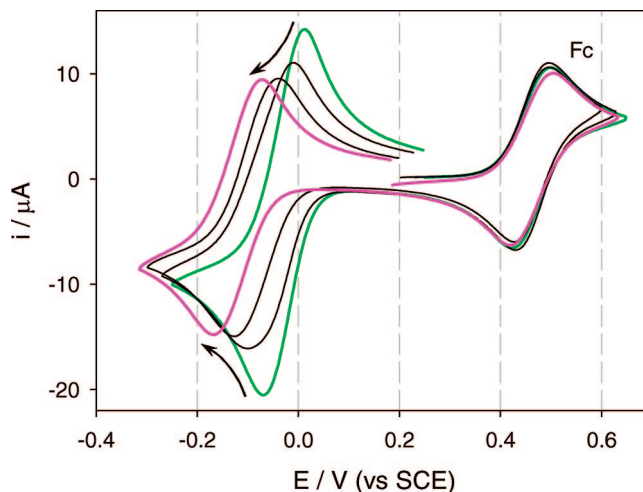
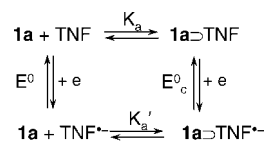


FIGURE 10. Cyclic voltammograms of TNF ($c = 1.2$ mM) upon addition of from 0 (green line) up to 2.0 (pink line) equiv of clip **1a** in $\text{CH}_2\text{Cl}_2/\text{TBAPF}_6$ solution. Working electrode, glassy carbon; scan rate, 0.05 V/s. Ferrocene (Fc) reversible oxidation is also reported.

SCHEME 5. Square Scheme Representing Formation of the **1a**⊃TNF Complex and the Reduction Processes



line in Figure 9b), compared to the cyclic voltammograms of the two separated components. The fact that the benzo-[k]fluoranthene moiety is more difficult to oxidize and TNF is more difficult to reduce when they are associated with one another demonstrates the charge transfer character of this complex. Moreover, lower current intensities are registered for **1a**⊃TNF because of the lower diffusion coefficient of the complex compared to the separated components. Indeed, the first oxidation process of **1a**⊃TNF is superimposed to the second oxidation process of the clip, but the current intensity is not doubled (Figure 9a). On the other hand, successive reduction and oxidation processes occur at the same potentials of the isolated components because upon one-electron oxidation or one-electron reduction, the complex is destroyed.

A more careful investigation of the cathodic region and, in particular, of the first process has been performed because of its complete chemical reversibility. Under the experimental conditions used in the experiments reported in Figure 9, the percentage of association is above 90%, estimated on the basis of the association constant measured in chloroform solution by photophysical data. By successive addition (from 0.5 to 3 equiv) of clip **1a** to a 1.2 mM solution of TNF, a progressive shift of the first reduction process is observed (Figure 10): the maximum shift of the half-wave potential compared to the free TNF is 95 mV, registered upon addition of 2 equiv of clip per guest molecule. Moreover, upon addition of clip **1a** to a TNF solution, a broadening and intensity decrease is observed (Figure 10), demonstrating that the diffusion coefficient (vide supra) and the rate of heterogeneous electron transfer is lower in the complex since the electroactive guest is encapsulated inside the cavity of the host.

The observed electrochemical behavior can be rationalized on the basis of the square scheme reported in Scheme 5, in which the association constant K_a of **1a** and TNF is much larger than that of **1a** and $\text{TNF}^{\cdot-}$ (K_a'). The two constants, K_a and K_a' , are linked by the following equation:²⁶

$$\ln\left(\frac{K_a}{K_a'}\right) = \frac{F(E^0 - E^0_C)}{RT} \quad (4)$$

where E^0 and E^0_C are the standard reduction potentials for TNF and **1a**⊃TNF, respectively. A good estimation of these values are the $E_{1/2}$ values reported in Table 5, from which the ratio K_a/K_a' results are of the order of 40.

Upon variation of the scan rate in the range 0.05–20 V/s, no change in the shape of the cyclic voltammogram is observed, indicating that both the forward and backward scan of the first reduction process are due to the redox couple **1a**⊃TNF/**1a**⊃TNF $^{\cdot-}$. The heterogeneous electron transfer rates are, in any case, higher than the association and dissociation rate constants of the complex between **1a** and TNF or **1a** and TNF $^{\cdot-}$.

Conclusions

Molecular clips (**1**) containing two extended aromatic sidewalls, namely, two benzo[*k*]fluoranthene units, linked by a dimethylene-bridged spacer unit containing a benzene ring substituted with two acetoxy (**1a**), hydroxy (**1b**), or methoxy (**1c**) groups in the para position, have been synthesized and fully characterized (NMR spectra, single-crystal structures, photophysical and electrochemical properties). These clips are strongly fluorescent, and anisotropy measurements demonstrate that fluorescence depolarization takes place by a very fast (subns) energy migration between the two identical benzo[*k*]fluoranthene units and, in fluid solution, by rotation of the clip. For the purpose of comparison, similar compounds (**2** and **3**), containing only one benzo[*k*]fluoranthene unit, have been prepared and studied.

The highly negative electrostatic potential on the inner cavity of these clips constitutes the recognition site for electron-deficient guest molecules. The effect on the association constants of (i) the presence of one or two identical aromatic sidewalls, (ii) different substituents on the bridging unit, and (iii) the nature of the aromatic sidewalls have been investigated with a variety of electron-acceptor molecules. In the case of polycyclic guests, clips **1** evidence hosting ability stronger than the corresponding anthracene and naphthalene clips (**4** and **5**). This finding can be rationalized with the larger van der Waals contact surface of the benzo[*k*]fluoranthene compared to the anthracene or naphthalene sidewalls.

Among the investigated systems, the most stable complex is that of clip **1a** with 9-dicyanomethylene-2,4,7-trinitrofluorene guest. The association constant ($K_a \approx 10^5 \text{ M}^{-1}$, in chloroform solution) has been estimated by spectrophotometric and spectrofluorimetric titrations. Indeed, profound changes of the photophysical properties are brought about by the formation of the complex **1a**⊃TNF: the presence of a new charge-transfer state is demonstrated by the presence of a broad absorption band at 600 nm and the quenching of the strong benzo[*k*]fluoranthene emission. Moreover, the electrochemical investigation shows a positive shift of the clip oxidation process and a concomitant negative shift of the TNF reduction process in the complex, while further reduction and oxidation processes are unaffected.

Therefore, the complex **1a**⊃TNF can be disassembled by electrochemical stimuli.

Experimental Section

Synthesis. Dimethoxy-benzo[*k*]fluoranthene Clip (1c). A Schlenk flask was equipped with a magnetic stirring bar, $\text{Pd}_2(\text{dba})_3$ (0.33 g, 0.37 mmol, dba = dibenzylidene acetone, $\text{Ph}-\text{CH}=\text{CH}-\text{C}(=\text{O})-\text{CH}=\text{CH}-\text{Ph}$), $\text{P}(\text{Cy})_3$ (0.55 g, 1.95 mmol, tricyclohexylphosphine, $\text{P}(c\text{-C}_6\text{H}_{11})_3$), (0.87 g, 1.11 mmol) **5d**, 1-naphthaleneboronic acid (0.5 g, 2.91 mmol), and DBU (2.5 mL, 1,8-diazabicyclo[5.4.0]undec-7-ene) in DMF (33 mL). The resulting mixture was stirred at 155 °C for 48 h. After dilution with 50 mL of CH_2Cl_2 , the mixture was washed three times with 50 mL of HCl (5%) and once with 50 mL of saturated NaHCO_3 and 50 mL of H_2O . Drying the organic phase over Na_2SO_4 and evaporation of the solvent gave the crude product. Column chromatography on silica gel, eluting with EtOAc/cyclohexane (1:3) yielded **1c** as a yellow solid (150 mg, 0.21 mmol, 19%); mp >240 °C (dec); $^1\text{H NMR}$ (CDCl_3 , 500 MHz) δ [ppm] 2.49 (br dt, 2H, $^2J(27i\text{-H}, 27a\text{-H}) = 7.15 \text{ Hz}$, 27a-H, 28a-H), 2.59 (br dt, 2H, 27i-H, 28i-H), 3.91 (s, 6H, $-\text{CH}_3$), 4.61 (br t, 4H, 9-H, 11-H, 22-H, 24-H), 7.54 (dd, 4H, $^3J(1\text{-H}, 2\text{-H}) = 7 \text{ Hz}$, $^3J(2\text{-H}, 3\text{-H}) = 8.05 \text{ Hz}$, 2-H, 5-H, 15-H, 18-H), 7.65 (s, 4H, 8-H, 12-H, 21-H, 25-H), 7.72 (d, 4H, 3-H, 4-H, 16-H, 17-H), 7.83 (d, 4H, 1-H, 6-H, 14-H, 19-H), 8.03 (s, 4H, 7-H, 13-H, 20-H, 26-H); $^{13}\text{C NMR}$ (CDCl_3 , 125 MHz) δ [ppm] 47.8 (C-9, C-11, C-22, C-24), 61.6 ($-\text{OCH}_3$), 64.5 (C-27, C-28), 119.0 (C-1, C-6, C-14, C-19), 120.3 (C-7, C-13, C-20, C-26), 120.6 (C-8, C-12, C-21, C-25), 126.0 (C-3, C-4, C-16, C-17), 128.1 (C-2, C-5, C-15, C-18), 130.4 (C-3a, C-16a), 132.2 (C-7a, C-12a, C-20a, C-25a), 134.8 (C-3c, C-16c), 137.1 (C-6a, C-13b, C-19a, C-26b), 137.4 (C-6b, C-13a, C-19b, C-26a), 139.9 (C-9a, C-10a, C-22a, C-23a), 145.7 (C-10, C-23), 147.8 (C-8a, C-11a, C-21a, C-24a); IR (KBr) $\tilde{\nu}$ [cm^{-1}] 3044 (C–H), 2992 (C–H), 2960 (C–H), 2926 (C–H), 2852 (C–H), 1477 (C=C), 1287 (C–O); UV–vis (CHCl_3) λ_{max} [nm] (log ϵ) 246 (4.77), 312 (4.75), 362 (3.87), 382 (4.07), 405 (4.09); MS (70 eV) m/z (%) 714 (100) [M^+], 699 (25) [$\text{M}^+ - \text{CH}_3$]; HR-MS (70 eV) found 714.2604; 714.2559 calcd for $\text{C}_{54}\text{H}_{34}\text{O}_2$.

Hydroquinone Benzo[*k*]fluoranthene Clip (1b). Under argon, a stirred solution of **1c** (198 mg, 0.28 mmol) in dichloromethane (25 mL) was cooled down to -78 °C and treated with boron tribromide (700 μL , 7.27 mmol). The solution was allowed to warm up slowly to room temperature over 24 h. Methanol (5 mL) was slowly added to the solution, which was cooled again with ice/water, to quench the excess of boron tribromide. After removal of the solvents the red-brown crude product was suspended in methanol, filtered and washed with 1 mL of acetonitrile. **1b** (159 mg, 0.23 mmol, 84%) was isolated as a brown-orange solid; mp > 300 °C; $^1\text{H NMR}$ ($\text{DMSO-}d_6$, 500 MHz) δ [ppm] 2.32 (br dt, 2H, $^2J(27i\text{-H}, 27a\text{-H}) = 8.40 \text{ Hz}$, 27a-H, 28a-H), 2.40 (br dt, 2H, 27i-H, 28i-H), 4.60 (br t, 4H, 9-H, 11-H, 22-H, 24-H), 7.62 (dd, 4H, $^3J(1\text{-H}, 2\text{-H}) = 6.90 \text{ Hz}$, $^3J(2\text{-H}, 3\text{-H}) = 8.15 \text{ Hz}$, 2-H, 5-H, 15-H, 18-H), 7.69 (s, 4H, 8-H, 12-H, 21-H, 25-H), 7.82 (d, 4H, 3-H, 4-H, 16-H, 17-H), 8.00 (d, 4H, 1-H, 6-H, 14-H, 19-H), 8.23 (s, 4H, 7-H, 13-H, 20-H, 26-H), 8.64 (2, 2H, -OH); $^{13}\text{C NMR}$ ($\text{DMSO-}d_6$, 125.7 MHz) δ [ppm] 46.4 (C-9, C-11, C-22, C-24), 64.2 (C-27, C-28), 119.5 (C-1, C-6, C-14, C-19), 120.0 (C-8, C-12, C-21, C-25), 120.4 (C-7, C-13, C-20, C-26), 125.9 (C-3, C-4, C-16, C-17), 128.3 (C-2, C-5, C-15, C-18), 129.9 (C-3a, C-16a), 131.5 (C-7a, C-12a, C-20a, C-25a), 133.7 (C-3a 1 , C-16a 1), 133.9 (C-9a, C-10a, C-22a, C-23a), 136.1 (C-6b, C-13a, C-19b, C-26a), 136.3 (C-6a, C-13b, C-19a, C-26b), 139.1 (C-10, C-23), 148.2 (C-8a, C-11a, C-21a, C-24a); IR (KBr) $\tilde{\nu}$ [cm^{-1}] 3338 (O–H), 3042 (C–H), 2991 (C–H), 2936 (C–H), 2862 (C–H), 1485 (C=C), 1277 (C–O); UV–vis (CHCl_3) λ_{max} [nm] (log ϵ) 252 (4.74), 309 (4.80), 362 (4.02), 382 (4.22), 405 (4.27); MS (70 eV) m/z (%) 686 (45) [M^+]; HR-MS (ESI+) m/z 709.2083 found; 709.2138 calcd for $\text{C}_{52}\text{H}_{30}\text{O}_2\text{N}_2$.

Diacetoxy Benzo[*k*]fluoranthene Clip (1a). Freshly distilled acetic anhydride (1.9 mL, 20.09 mmol) was added under argon to

a stirred solution of **1b** (120 mg, 0.17 mmol) in pyridine (23 mL). The solution was stirred for 24 h at room temperature and then poured into ice–water (100 mL). The precipitate was filtered, washed with water, and dried over P₂O₅. Purification by column chromatography on silica gel with a mixture of EtOAc/cyclohexane (1:3) as eluent gave **1a** (107 mg, 0.139 mmol, 82%) as a yellow solid: mp > 300 °C; ¹H NMR (CDCl₃, 500 MHz) δ [ppm] 2.51 (br dt, 2H, ²J(27i-H, 27a-H) = 7.95 Hz, 27i-H, 28i-H), 2.56 (s, 6H, -CH₃), 2.72 (br dt, 2H, 27a-H, 28a-H), 4.36 (br t, 4H, 9-H, 11-H, 22-H, 24-H), 7.52 (dd, 4H, ³J(1-H, 2-H) = 6.90 Hz, ³J(2-H, 3-H) = 8.10 Hz, 2-H, 5-H, 15-H, 18-H), 7.61 (s, 4H, 8-H, 12-H, 21-H, 25-H), 7.70 (d, 4H, 3-H, 4-H, 16-H, 17-H), 7.78 (d, 4H, 1-H, 6-H, 14-H, 19-H), 7.95 (s, 4H, 7-H, 13-H, 20-H, 26-H); ¹³C NMR (CDCl₃, 125.7 MHz) δ [ppm] 21.1 (-CH₃), 48.4 (C-9, C-11, C-22, C-24), 65.1 (C-27, C-28), 118.9 (C-1, C-6, C-14, C-19), 120.2 (C-7, C-13, C-20, C-26), 121.2 (C-8, C-12, C-21, C-25), 125.9 (C-3, C-4, C-16, C-17), 128.1 (C-2, C-5, C-15, C-18), 130.4 (C-3a, C-16a), 132.3 (C-7a, C-12a, C-20a, C-25a), 134.8 (C-3a¹, C-16a¹), 137.1 (C-6a, C-13b, C-19a, C-26b), 137.3 (C-6b, C-13a, C-19b, C-26a), 137.5 (C-10, C-23), 141.0 (C-9a, C-10a, C-22a, C-23a), 146.3 (C-8a, C-11a, C-21a, C-24a), 168.8 (C=O); IR (KBr) $\tilde{\nu}$ [cm⁻¹] 3044 (C–H), 2989 (C–H), 2936 (C–H), 2857 (C–H), 1763 (C=O), 1205 (C–O); UV–vis (CHCl₃) λ_{\max} [nm] (log ϵ) 247 (5.09), 314 (5.10), 362 (4.10), 384 (4.22), 405 (4.24); MS (70 eV) *m/z* (%) 770 (100) [M⁺], 728 (38) [M⁺ – CH₂CO], 686 (65) [M⁺ – 2·CH₂CO]; HR-MS (ESI+) found 793.2351; 793.2349 calcd for C₅₆H₃₄O₄Na.

8,9-Bis(dibromomethyl)fluoranthene (6). A reaction vessel (quartz glass) equipped with a photolysis lamp (150 W mercury high-pressure lamp) was charged with 8,9-dimethylfluoranthene (4.48 g, 19.45 mmol), *N*-bromosuccinimide (15.20 g, 85.40 mmol), and 200 mL of CCl₄. The reaction started by heating the stirred mixture to reflux under irradiation for 36 h. The reaction mixture was cooled down to room temperature, and the precipitate consisting of insoluble succinimide and of product only slightly soluble in CCl₄ was filtered off. The soluble portion of the product was in the filtrate. The succinimide was dissolved in water by extraction of the filtered solid. The remaining solid insoluble in water contained the major portion of the product, which was dissolved in chloroform. The filtrate and the chloroform solution were worked up separately. To remove the excess of bromine, the organic phases were washed with saturated aqueous NaHSO₃ solution. After washing with water several times the organic phases were dried over MgSO₄ and evaporation of the solvent gave product **6** (10.36 g, 18.98 mol, 98%) as a light yellow solid: mp > 170 °C (dec); ¹H NMR (CDCl₃, 500 MHz) δ [ppm] 7.30 (br s, 2H, 11-H, 12-H), 7.71 (dd, 2H, *J*(2-H, 1-H) = 6.95 Hz, *J*(2-H, 3-H) = 8.20 Hz, 2-H, 5-H), 7.94 (d, 2H, 3-H, 4-H), 8.05 (d, 2H, 1-H, 6-H), 8.21 (br s, 2H, 7-H, 10-H); ¹³C NMR (CDCl₃, 125.7 MHz) δ [ppm] 37.3 (C-11, C-12), 121.8 (C-1, C-6), 128.2 (C-3, C-4), 128.3 (C-2, C-5), 130.2 (C-3a), 133.4 (C-3a¹), 135.1 (C-6a, C-10b); IR (KBr) $\tilde{\nu}$ [cm⁻¹] 3045 (C–H), 2997 (C–H), 1460 (C=C), 665 (C–Br); UV–vis (CHCl₃) λ_{\max} [nm] (log ϵ) 246 (4.52), 262 (4.35), 296 (4.45), 332 (3.87), 365 (4.09), 373 (4.11); MS (70 eV) *m/z* (%) = 546 (3) [M⁺], 466 (15) [M⁺ – Br], 386 (20) [M⁺ – 2·Br], 307 (30) [M⁺ – 3·Br], 226 (100) [M⁺ – 4·Br], isotopic pattern: *m/z* (%) 541.7517 (15), 543.7497 (67), 545.7477 (100), 547.7469 (70), 549.7442 (15); HR-MS (70 eV) found 545.7477; 545.7476 calcd for C₁₈H₁₀Br₄.

“Half-Clip” (9a). A mixture of bisdienophile **8a** (0.99 g, 2.97 mmol), 8,9-bis(dibromomethyl)fluoranthene **6** (5.48 g, 10.0 mmol), anhydrous NaI (9.41 g, 62.78 mmol), anhydrous CaCO₃ (2.05 g, 20.32 mmol), and anhydrous DMF (72 mL) was stirred under argon for 30 min at room temperature and then heated to 55 °C under vacuum (100 mbar) for 5 h. The reaction mixture was poured into ice (300 g), the brown mixture was, after decolorization by addition of aqueous sodium hydrogen sulfite, extracted with dichloromethane (3 × 200 mL), and the combined organic layers were filtered, washed with saturated aqueous sodium hydrogen carbonate (2 × 150 mL) and water (2 × 150 mL), dried over Na₂SO₄, and

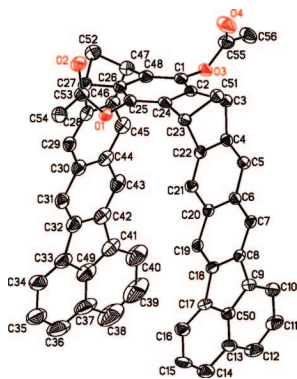
concentrated in vacuo in a rotary evaporator. Purification by column chromatography on silica gel with a mixture of EtOAc/cyclohexane (1:3) as eluent gave **9a** (460 mg, 0.84 mmol, 28%) as a light yellow solid: mp 212 °C; ¹H NMR (CDCl₃, 500 MHz) δ [ppm] 2.20 (dt, 1H, ²J(20i-H, 20a-H) = 6.90 Hz, 20i-H), 2.26 (dt, 1H, 20a-H), 2.44 (s, 6H, -CH₃), 2.51 (dt, 1H, ²J(19i-H, 19a-H) = 8.10 Hz, 19i-H), 2.69 (dt, 1H, 19a-H), 3.81 (m, 2H, 11-H, 14-H), 4.35 (br t, 2H, 9-H, 16-H), 6.65 (m, 2H, 12-H, 13-H), 7.63 (dd, 2H, ³J(1-H, 2-H) = 6.9 Hz, ³J(2-H, 3-H) = 8.15 Hz, 2-H, 5-H), 7.70 (s, 2H, 8-H, 17-H), 7.80 (d, 2H, 3-H, 4-H), 7.93 (d, 2H, 1-H, 6-H), 8.16 (s, 2H, 7-H, 18-H); ¹³C NMR (CDCl₃, 125.7 MHz) δ [ppm] 21.0 (-CH₃), 48.0 (C-9, C-16), 48.3 (C-11, C-14), 65.3 (C-19), 69.7 (C-20), 119.1 (C-1, C-6), 120.5 (C-7, C-18), 121.1 (C-8, C-17), 126.1 (C-3, C-4), 128.2 (C-2, C-5), 130.6 (C-3a), 132.4 (C-7a, C-17a), 135.0 (C-3a¹), 137.4 (C-6a, C-18b), 137.5 (C-6b, C-18a), 137.6 (C-10a, C-14a), 140.2 (C-9a, C-15a), 142.8 (C-12, C-13), 143.2 (C-10, C-23), 146.9 (C-8a, C-16a), 169.0 (C=O); IR (KBr) $\tilde{\nu}$ [cm⁻¹] 2989 (C–H), 2936 (C–H), 2867 (C–H), 1762 (C=O), 1203 (C–O); UV–vis (CHCl₃) λ_{\max} [nm] (log ϵ) 245 (4.66), 309 (4.67), 359 (3.96), 379 (4.03), 403 (3.99); MS (70 eV) *m/z* (%): 546 (45) [M⁺], 504 (12) [M⁺ – CH₂CO], 462 (27) [M⁺ – 2·CH₂CO]; HR-MS (ESI+) found 569.1728; 569.1723 calcd for C₃₈H₂₆NaO₄.

Diacetoxy Clip with One Benzo[*k*]fluoranthene and One Naphthalene Sidewall (2a). A mixture of **9a** (250 mg, 0.46 mmol), *o*-bis(dibromomethyl)benzene (1.16 g, 2.75 mmol), anhydrous NaI (3.5 g, 23.35 mmol), anhydrous CaCO₃ (0.79 g, 7.89 mmol), and anhydrous DMF (20 mL) was stirred under argon for 30 min at room temperature and then heated to 55 °C under vacuum (100 mbar) for 5 h. The reaction mixture was poured into ice (100 g), the brown mixture was, after decolorization by addition of aqueous sodium hydrogen sulfite, extracted with dichloromethane (3 × 75 mL), and the combined organic layers were filtered, washed with saturated aqueous sodium hydrogen carbonate (2 × 75 mL) and water (2 × 75 mL), dried over Na₂SO₄, and concentrated in vacuo in a rotary evaporator. Purification by column chromatography on silica gel with a mixture of EtOAc/cyclohexane (1:3) as eluent gave **2a** (150 mg, 0.23 mmol, 51%) as a light yellow solid: mp > 300 °C; ¹H NMR (CDCl₃, 500 MHz) δ [ppm] 2.44, 2.49 (2dt, 2H, ²J(23i-H, 23a-H) = 7.95 Hz, 23a-H, 24a-H), 2.51 (s, 6H, -CH₃), 2.68, 2.71 (m, 2H, 23i-H, 24i-H), 4.32 (br t, 2H, 11-H, 18-H or 9-H, 20-H), 4.33 (br t, 2H, 11-H, 18-H or 9-H, 20-H), 7.21 (m, 2H, 14-H, 15-H), 7.53 (s, 2H, 12-H, 17-H), 7.55 (m, 2H, 13-H, 16-H), 7.59 (dd, 2H, ³J(2-H, 3-H) = 8.10 Hz, ³J(2-H, 1-H) = 6.90 Hz, 2-H, 5-H), 7.64 (s, 2H, 8-H, 21-H), 7.76 (d, 2H, 3-H, 4-H), 7.88 (d, 2H, 1-H, 6-H), 8.06 (s, 2H, 7-H, 22-H); ¹³C NMR (CDCl₃, 125.7 MHz) δ [ppm] 21.1 (-CH₃), 48.2, 48.4 (C-9, C-11, C-18, C-20), 65.2 (C-23, C-24), 119.0 (C-1, C-6), 120.2 (C-12, C-17), 120.4 (C-7, C-22), 121.2 (C-8, C-21), 125.4 (C-14, C-15), 126.0 (C-3, C-4), 127.8 (C-13, C-16), 128.2 (C-2, C-5), 130.5 (C-3a), 132.28 (C-12a, C-16a), 132.33 (C-7a, C-21a), 134.9 (C-3a¹), 137.29 (C-6a, C-22b), 137.40 (C-6b, C-22a), 137.41 (C-10, C-19), 140.9 (C-9a, C-10a, C-18a, C-19a), 145.9 (C-11a, C-17a), 146.4 (C-8a, C-20a), 168.8 (C=O); IR (KBr) $\tilde{\nu}$ [cm⁻¹] 2963 (C–H), 2931 (C–H), 2858 (C–H), 1762 (C=O), 1198 (C–O); UV–vis (CHCl₃) λ_{\max} [nm] (log ϵ) 243 (4.82), 315 (4.77), 362 (3.91), 382 (4.05), 405 (4.05); MS (70 eV) *m/z* (%) 646 (100) [M⁺], 604 (60) [M⁺ – CH₂CO], 562 (100) [M⁺ – 2·CH₂CO]; HR-MS (ESI+) found 669.2086; 669.2036 calcd for C₄₆H₃₀NaO₄.

Diacetoxy Benzo[*k*]fluoranthene “Half-Clip” (3a). A mixture of dienophile **10a** (214 mg, 0.83 mmol), 8,9-bis(dibromomethyl)fluoranthene **6** (1.53 g, 2.8 mmol), anhydrous NaI (2.62 g, 17.48 mmol), anhydrous CaCO₃ (0.57 g, 5.69 mmol), and anhydrous DMF (20 mL) was stirred under argon for 30 min at room temperature and then heated to 55 °C under vacuum (100 mbar) for 5 h. The reaction mixture was poured into ice (120 g), the brown mixture was, after decolorization by addition of aqueous sodium hydrogen sulfite, extracted with dichloromethane (3 × 100 mL), and the combined organic layers were filtered, washed with saturated aqueous sodium hydrogen carbonate (2 × 100 mL) and water (2

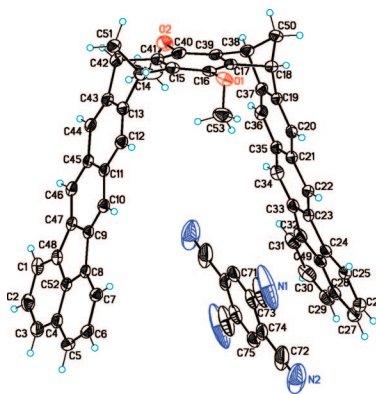
× 100 mL), dried over Na₂SO₄, and concentrated in vacuo in a rotary evaporator. Purification by column chromatography on silica gel with a mixture of EtOAc/cyclohexane (1:3) as eluent gave **3a** (150 mg, 0.31 mmol, 38%) as a light yellow solid: mp 201 °C; ¹H NMR (CDCl₃, 500 MHz) δ [ppm] 2.42 (s, 6H, -CH₃), 2.53 (br dt, 1H, ²J(17i-H, 17a-H) = 8.00 Hz, 17i-H), 2.68 (br dt, 1H, 17a-H), 4.45 (br t, 2H, 9-H, 14-H), 6.72 (s, 2H, 11-H, 12-H), 7.64 (dd, 2H, ³J(1-H, 2-H) = 7 Hz, ³J(2-H, 3-H) = 8 Hz, 2-H, 5-H), 7.79 (s, 2H, 8-H, 15-H), 7.81 (d, 2H, 3-H, 4-H), 7.95 (d, 2H, 1-H, 6-H), 8.2 (s, 2H, 7-H, 16-H); ¹³C NMR (CDCl₃, 125.7 MHz): π [ppm] 21.1 (-CH₃), 48.9 (C-9, C-14), 64.3 (C-17), 119.2 (C-1, C-6), 120.3 (C-11, C-12), 120.5 (C-7, C-16), 121.7 (C-8, C-15), 126.1 (C-3, C-4), 128.3 (C-2, C-5), 130.6 (C-3a), 132.4 (C-7a, C-15a), 135.0 (C-3a'), 137.3 (C-6a, C-16b), 137.6 (C-6b, C-16a), 142.5 (C-10, C-13), 142.8 (C-9a, C-13a), 145.9 (C-8a, C-14a), 169.1 (C=O); IR (KBr) $\tilde{\nu}$ [cm⁻¹] 3040 (C-H), 3002 (C-H), 2939 (C-H), 2872 (C-H), 1759 (C=O), 1187 (C-O); UV-vis (CHCl₃) λ_{max} [nm] (log ϵ) 247 (4.62), 309 (4.63), 362 (3.92), 380 (4.01), 405 (3.97); MS (70 eV) *m/z* (%): 482 (45) [M⁺], 440 (30) [M⁺ - CH₂CO], 398 (100); HR-MS (ESI⁺): found 505.1381; 505.1410 calcd for C₃₃H₂₂NaO₄.

Crystal Structure Determinations. **1a**·2CHCl₃·C₅H₃₂·2CHCl₃, crystal dimensions 0.24 × 0.21 × 0.07 mm; crystal color, yellow. *T* = 183(2) K. Cell dimensions *a* = 14.9970(7), *b* = 16.5112(8), *c* = 20.8902(10) Å, α = 89.845(3)°, β = 77.689(3)°, γ = 69.656(2)°, *V* = 4724.2(4) Å³, triclinic crystal system, *Z* = 4, *d*_{calcd} = 1.424 g cm⁻³, μ = 0.414 mm⁻¹, space group *P* $\bar{1}$, data collection of 137606 intensities, 9198 independent (*R*_{merg} = 0.0855, 1.49° = Θ = 20.34°), 5839 observed [*F*_o ≥ 4σ(*F*)], Data reduction and absorption correction with Bruker AXS APEX2 Vers. 10-27 2005 program multiscan. *R*_{merg} before/after: 0.0853/0.0503, max/min transmission 0.97/0.85; structure solution with direct methods (SHELXS) and refinement on *F*² (SHELXTL 6.12) (1288 parameters), the hydrogen atom positions were calculated and refined as riding models on idealized geometries with the 1.2-fold (1.5-fold for methyl groups) isotropic displacement parameters of the equivalent Uij of the corresponding carbon atoms. The trichloromethane atoms Cl(1) to Cl(3) and Cl(10) to Cl(12) are disordered over two sites with SOF 0.8 and 0.2. Further disorder was detected at the oxygen atom O6 at two sites with SOF 0.6 and 0.4. The poor *R*-values and residual electron density resulted from nonresolved disorder and poor crystal quality. Therefore, the results are taken for a confirmation of the overall molecular geometry and packing mode. *R*₁ = 0.0915, *wR*₂ (all data) = 0.2205, maximum residual electron density 0.954 e Å⁻³.



1c·1/2C₁₀H₂N₄·2CHCl₃·C₅H₃₄·1/2 C₁₀H₂N₄·2CHCl₃, crystal dimensions 0.17 × 0.14 × 0.11 mm, crystal color, orange. *T* = 203(2) K. Cell dimensions *a* = 34.167(3), *b* = 14.8708(15), *c* = 22.173(2) Å, β = 117.776(2)°, *V* = 9967.8(17) Å³, monoclinic crystal system, *Z* = 8, *d*_{calcd} = 1.390 g cm⁻³, μ = 0.393 mm⁻¹, space group *C*2/*c*, data collection of 64258 intensities, 12403 independent (*R*_{merg} = 0.0865, 1.66° = Θ = 28.35°), 4948 observed [*F*_o ≥ 4σ(*F*)], Data reduction and absorption correction with Bruker AXS APEX2 Vers. 10-27 2005 program multiscan. *R*_{merg} before/

after: 0.0753 / 0.0552, max/min transmission 1.00/0.89; structure solution with direct methods (SHELXS) and refinement on *F*² (SHELXTL 6.12) (641 parameters), the hydrogen atom positions were calculated and refined as riding models on idealized geometries with the 1.2-fold (1.5-fold for methyl groups) isotropic displacement parameters of the equivalent Uij of the corresponding carbon atoms. The ADPs of the atoms C12, C13, C15, N1, N2, c71 and C72 indicate some disorder which was not resolved. *R*₁ = 0.0818, *wR*₂ (all data) = 0.2122, maximum residual electron density 0.818 e Å⁻³.



Determination of *K*_a by Solid-liquid Extraction Experiments. See Supporting Information.

Determination of *K*_a by ¹H NMR Titration Method. See ref 3a.

The results of all titration experiments are given in the Supporting Information.

The estimated experimental error on the association constant is 15%. The errors result from standard deviation of the nonlinear regression.²⁴

Photophysics. The experiments were carried out in air-equilibrated CHCl₃ solution at 298 K. Global fitting of absorption and emission spectra has been performed by SPECFIT software.²³ The fluorescent decay curves were collected under 0° and 90° polarization angles. Global analysis on fluorescence anisotropy decay curves has been performed by FAST software (version 1.8.1). The estimated experimental errors are 2 nm on the band maximum, 5% on the molar absorption coefficient, fluorescence lifetime, steady-state fluorescence anisotropy at 298 K and log*K* values, 10% on the fluorescence quantum yield, and 15% on rotational correlation times, and steady-state fluorescence anisotropy at 77 K.

Electrochemistry. The electrochemical experiments were carried out in argon-purged CH₂Cl₂ solution at 298 K. In the cyclic voltammetry (CV) the working electrode was a glassy carbon electrode (0.08 cm²), the counter electrode was a Pt spiral, and a silver wire was employed as a quasi-reference electrode (AgQRE). The potentials reported are referred to SCE by measuring the AgQRE potential with respect to ferrocene (*E*_{1/2} = 0.46 V vs SCE for Fc⁺/Fc). The concentration of the compounds examined was of the order of 1 × 10⁻³ M; 0.1 M tetrabutylammonium hexafluorophosphate (TBAPF₆) was added as supporting electrolyte. Cyclic voltammograms were obtained with scan rates in the range 0.05–20 V s⁻¹. The estimated experimental error on the *E*_{1/2} value is ±10 mV.

Acknowledgment. This work has been supported in Italy by MIUR (PRIN 2006034123_003) and in Germany by the “Deutsche Forschungsgemeinschaft” (DFG, KL 299/13-1). We thank Heinz Bandmann and Dr. Torsten Schaller for NMR measurements, Willi Sicking for assistance with the HOSTEST calculations, and Professor Craig Wilcox for providing us access to the HOSTEST program.

Supporting Information Available: General experimental details. ^1H NMR spectra of the new compounds. Pdb files containing atom coordinates for the calculated structures. Experimental data for the determination of association constants K_a and complexation-induced chemical ^1H NMR shifts, $\Delta\delta_{\text{max}}$, by ^1H NMR titrations. CCDC-682029 (for **1a**•2CHCl₃) and CCDC-682030 (for **1c**•1/2C₁₀H₂N₄•2CHCl₃) contain the supplementary crystallographic data for this paper.

These data can be obtained free of charge at www.ccdc.cam.ac.uk/conts/retrieving.html [or from the Cambridge Crystallographic Data Centre, 12 Union Road, Cambridge CB2 1EZ, UK. Fax: +44-1223-336-033. E-mail: deposit@ccdc.cam.ac.uk]. This material is available free of charge via the Internet at <http://pubs.acs.org>.

JO8007513